Nano Research
DOI 10.1007/s12274-015-0956-y
Research Article
ISSN 1998-0124
CN 11-5974/O4

Topological to trivial insulating phase transition in stanene

Michel Houssa[1] (✉), Bas van den Broek[2], Konstantina Iordanidou[1], Augustin Lu[1,2], Geoffrey Pourtois[2], Jean-Pierre Locquet[1], Valery Afanas'ev[1], and Andre Stesmans[1]

Nano Res., **Just Accepted Manuscript** • DOI: 10.1007/s12274-015-0956-y
http://www.thenanoresearch.com on November. 15, 2015

Just Accepted

Topological to trivial insulating phase transition in stanene

M. Houssa[(a)], B. van den Broek[(a)], K. Iordanidou[(a)], A. Lu[(a,b)], G. Pourtois[(b)],

J.P. Locquet[(a)], V.V. Afnanas'ev[(a)] and A. Stesmans[(a)]

[(a)]Department of Physics and Astronomy, University of Leuven,

Celestijnenlaan 200D, B-3001 Leuven, Belgium

[(b)]imec, 75 Kapeldreef, B-3001 Leuven, Belgium

Corresponding author:

Michel Houssa, michel.houssa@fys.kuleuven.be

Abstract

The electronic properties of stanene, the Sn counterpart of graphene, are theoretically studied using first-principles simulations. A topological to trivial insulating phase transition, either induced by an out-of-plane electric field or by quantum confinement effects is predicted. These results highlight the potential use of stanene nanoribbons in gate-voltage controlled dissipationless spin-based devices, and also set the minimal nanoribbon width to be used in such devices, which should be typically about 5 nm.

Keywords: 2D materials, topological insulators, DFT simulations, Electronic structure

Two dimensional (2D) materials are gaining a lot of interest for their potential use in nanoelectronic devices, these materials offering the possibility to downscale the channel thickness at the atomic level, which could lead to much improved electrostatic control of the device and suppression of so-called short channel effects [1-3]. Among these materials, graphene could be used in high frequency analog devices [2,4] and semiconducting transition metal dichalcogenides could be integrated in high performance and low power logic devices [2,3,5]. Other group-IV 2D hexagonal layers like silicene [6-8], germanene [9] and stanene [10-15] are also gaining much interest, due to their predicted unique structural and electronic properties, as well as their possible better compatibility with the existing Si nanotechnology platform (as compared to graphene). Stanene, a two dimensional layer of Sn atoms, is predicted to be a topological insulator with an energy band gap of about 0.1 eV, which is induced by the strong spin orbit (SO) coupling in this 2D material [10-13]. Transport via spin-polarized edge states should then take place in stanene nanoribbons, potentially of much interest for future low-power (dissipationless) spin-based logic devices. Remarkably, the possible growth of stanene on (111)Bi_2Te_3 substrates has been reported very recently [14], paving the way to the potential use of this novel 2D material in low power spintronic devices.

Using first-principles calculations, based on density-functional theory (DFT), we report here the possibility to tune the electronic properties of stanene with an out-of-plane electric field, a transition from a topological to trivial insulator being predicted at a critical electric field of about 0.5 V/Å. The interplay between quantum confinement and spin orbit coupling effects on the topological order of stanene nanoribbons is next investigated. Our results highlight the importance of the minimal nanoribbon gate width in spin-based dissipationless devices, which should be about 5 nm.

DFT simulations were performed with the plane-wave code Quantum Espresso [16], using the generalized

gradient approximation for the exchange-correlation functional, as parametrized by Perdew-Burke-Enzerhoff (PBE) [17]. A fully relativistic projected augmented wave (PAW) pseudopotential was used [18], with a cut-off energy of 36 Ry. The k-point mesh for the Brillouin zone integration was fixed to (8x8x1) for the atomic relaxation and (20x20x1) for the computation of the energy band structure, with a convergence criteria fixed to 10^{-6} Ry. Quantum confinement effects were studied on Sn armchair nanoribbons, with different widths. The egdes of the ribbons were passivated by F atoms, the topological order of stanene being preserved when functionalized by F adatoms [10]. The computations were performed on periodic slab models, with a vacuum layer of about 10 Å to avoid spurious interactions between the neighbouring cells. To study the effect of an external electric field on the electronic properties of the system, a periodic saw-like potential was applied in the direction perpendicular to the slab.

The computed in-plane lattice parameter of stanene is 4.70 Å and its buckling distance is 0.82 Å, in very good agreement with previous DFT calculations [10-13]. Band inversion is induced by SO coupling, the material being a 2D topological insulator with a computed energy band gap (at the K-point) of about 0.1 eV, as shown in Fig. 1, also in agreement with previous calculations [10].

The effect of an out-of-plane electric field on the computed energy band structure of stanene is shown in Fig. 2. For an electric field lower than about 0.5 V/Å, one observes a decrease of the SO coupling-induced energy band gap at the K-point. When the electric field reaches about 0.5 V/Å, the gap closes at the K-point and the system becomes metallic. For an electric field higher than this critical value, the gap opens again, but in this case, band inversion does not occur and the material is a trivial insulator. The computed energy band-gap is shown in Fig. 3 as a function of the out-of-plane electric field E_z. A typical W shape is observed, characteristic of a transition from a topological insulator to a trivial insulator [19] at a critical field of about 0.5 V/Å.

This electronic phase transition is related to the breaking of the inversion symmetry by the presence of the

out-of-plane electric field and the occurrence of an (extrinsic) Rashba effect [20,21]. Within an effective tight-binding Hamiltonian approximation, the Rashba coupling constant λ_R is given by [20,21]

$$\lambda_R = \frac{eE_z z_0 \xi^2}{3V_{sp\sigma}} \quad , \qquad (1)$$

where e is the electron charge, E_z the amplitude of the out-of-plane electric field, $z_o=3a_o$, with a_o the Bohr radius, ξ the strength of the atomic spin-orbit interaction and $V_{sp\sigma}$ the nearest-neighbour hopping parameter between s and p orbitals of σ-type bonds; we used here ξ= 0.8 eV and $V_{sp\sigma}$=2.65 eV, as computed for stanene [22]. For a critical electric field E_z=0.5 V/Å, the corresponding Rashba coupling constant equals about 80 meV, which is close to the calculated spin-orbit coupling constant λ_{SO} of stanene (about 70 meV) [22]. Consequently, when $\lambda_R \approx \lambda_{SO}$, the energy gap vanishes at the K-point and the system becomes metallic. When $\lambda_R > \lambda_{SO}$, the system becomes a trivial insulator. This predicted electric field induced topological to trivial insulating phase transition in stanene is potentially very useful for gate voltage controlled dissipationless spin-based devices. Note that the critical electric field E_z=0.5 V/Å corresponds to a moderate (gate) voltage drop of about 0.4 V in the stanene layer, its thickness (Sn-Sn buckling distance) being about 0.8 Å.

We next investigated the effect of quantum confinements in stanene nanoribbons on the topological order of the system. A F-passivated armchair stanene nanoribbons with a width W=6 is shown in Fig. 4. Note that W represents the number of Sn dimer rows along the ribbon width, in the zig-zag direction [23]. The computed band gap of the Sn nanoribbons is shown in Fig.5 (a) as a function of W. Note that these results were obtained without including SO coupling in the calculations, and illustrate the energy gap induced in the nanoribbon by quantum confinements. In analogy with graphene, the computed energy band gaps of the Sn nanoribbons are oscillating

with W, with a typical periodicity of 3, corresponding to W=3m-1, W=3m and W=3m+1 (with m an integer) [23]. When SO coupling is included in the calculations, the energy gap also present oscillations, as shown in Fig. 5 (b). The results for W=3m and W=3m+1 are comparable to those obtained without SO coupling. In these systems (open squares in Fig. 5 (b)), quantum confinements lead to an energy gap typically larger than about 0.1 eV, and the material behaves like a trivial insulator (absence of band-inversion). The energy band structure of a W=6 nanoribbon (with SO coupling) is shown in Fig. 6(a). The absence of a Dirac cone in the band structure at the Γ-point (related to the spin-polarized edge states [10]) confirms that the system behaves like a trivial insulator. On the other hand, the W=3m-1 systems (full squares in Fig. 5 (b)) are predicted to be topological insulators. In these systems, the quantum-confinement induced band gap is typically smaller than about 0.1 eV, cf. Fig. 5 (a), and band-inversion does occur. As an example, the energy band structure of a W=8 nanoribbon is shown in Fig. 6 (b); one clearly observes a Dirac-like cone crossing the Fermi level at the Γ point, corresponding to the presence of spin-polarized edge states, as expected for a topological insulator [10]. Note that the energy gap is defined here as the difference between the "bulk" conduction and valence energy band at the Γ-point, as illustrated in Fig. 6 (b). We thus conclude that the topological order of stanene nanoribbons depends on W: nanoribbons with an energy gap E_G larger than typically 0.1 eV (induced by quantum confinements) behave like trivial insulators. When the quantum-confinement induced energy gap is lower than about 0.1 eV, the system is predicted to be a topological insulator, with spin-polarized edge-states. These findings highlight the importance of the width of the stanene nanoribbon to be potentially used in dissipationless spin-based devices: due to the band gap oscillations and inherent process-induced variation in the ribbon width, W should be larger than about 20, corresponding to a physical gate width of about 5 nm, in these devices.

Acknowledgments

Part of this work has been financially supported by the KU Leuven Research Funds, project GOA/13/011.

References

[1] Butler, S.Z.; *et al.* Progress, Challenges and opportunities in two-dimensional materials beyond graphene. *ACS Nano* **2013**, *7*, 2898-2926.

[2] Fiori, G.; Bonaccorso, F; Iannaccone, G.; Palacios, T.; Neumaier, D.; Seabaugh, A.; Banerjee, S.K.; Colombo, L. Electronics based on two-dimensional materials. *Nature Nanotechnol.* **2014**, *9*, 768-779.

[3] Schwierz, F.; Pezoldt, J.; Granzner, R. Two-dimensional materials and their prospects in transistor electronics. *Nanoscale* **2015**, *7*, 8261-8283.

[4] Lin, Y.M.; Dimitrakopoulos, C.; Jenkins, K.A.; Farmer, D.B.; Chiu, Y.H.; Grill, A.; Avouris, Ph. 100-GHz Transistors from Wafer-Scale Epitaxial Graphene. *Science* **2010**, *327*, 662.

[5] Kang, K.; Xie, S.; Huang, L.; Han, Y.; Huang, P.Y.; Mak, K.F.; Kim, C.J.; Muller, D.; Park, J. High-mobility three-atom-thick semiconducting films with wafer scale homogeneity. *Nature* **2015**, *520*, 656-660.

[6] Vogt, P.; De Padova, P.; Quaresima, C.; Avila, J.; Frantzeskakis, E.; Asensio, M.C.; Resta, A.; Ealet, B.; Le Lay, G. Silicene: Compelling experimental evidence for graphenelike two-dimensional silicon. *Phys. Rev. Lett.* **2012**, *108*, 155501.

[7] Tao, L.; Cinquanta, E.; Chiappe, D.; Grazianetti, C.; Fanciulli, M.; Dubey, M.; Molle, A.; Akinwande, D. Silicene field-effect transistors operating at room temperature. *Nature Nanotechnol.* **2015**, *10*, 227-231.

[8] Houssa, M.; Dimoulas, A.; Molle, A. Silicene: a review of recent experimental and theoretical investigations. *J. Phys.: Condens. Matter* **2015**, *27*, 253002-253020.

[9] Davilla, M.E.; Xian, L.; Cahangirov, S.; Rubio, A.; Le Lay, G. Germanene: a novel two-dimensional germanium allotrope akin to graphene and silicene. *New J. Phys.* **2014**, *16*, 095002.

[10] Xu, Y.; Yan, B.; Zhang, H.J.; Wang, J.; Xu, G.; Tang, P.; Duan, W.; Zhang, S.Z. Large-gap quantum spin Hall insulators in tin films, *Phys. Rev. Lett.* **2013**, *111*, 136804.

[11] Wu, S.C.; Shan, G.; Yan, B. Prediction of near-room-temperature quantum anomalous Hall effect on honeycomb materials. *Phys. Rev. Lett.* **2014**, *113*, 256401.

[12] Suarez Negreira, A.; Vandenberghe, W.G.; Fischetti, M.V. *Ab initio* study of the electronic properties and thermodynamic stability of supported and functionalized two-dimensional Sn films. *Phys. Rev. B* **2015**, *91*, 245103.

[13] van den Broek, B.; Houssa, M.; Scalise, E.; Pourtois, G.; Afanas'ev, V.V.; Stesmans, A. Two-dimensional hexagonal tin: *ab initio* geometry, stability, electronic structure and functionalization. *2D Materials* **2014**, *1*, 021004.

[14] Zhu, F.F.; Chen, W.J.; Xu, Y.; Gao, C.L.; Guan, D.D.; Liu, C.H.; Qian, D.; Zhang, S.C.; Jia, J.F. Epitaxial growth of two-dimensional stanene. *Nature Mater.* **2015**, *14*, 1020-1025.

[15] Xu, Y.; Tang, P.; Zhang, S.C. Large-gap quantum spin Hall states in decorated stanene grown on a substrate. *Phys. Rev. B* **2015**, *92*, 081112.

[16] Giannozzi, P.; *et al.* Quantum espresso: a modular and open-source software project for quantum simulations of materials. *J. Phys.: Condens. Matter* **2009**, *21*, 395502.

[17] Perdew, J.; Burke, K.; Ernzerhof, M. Generalized gradient approximation made simple. *Phys. Rev. Lett.* **1996**, *77*, 3865-3868.

[18] Blöchl, P.E. Projector augmented-wave method. *Phys. Rev. B* **1994**, *50*, 17953-17979.

[19] Ezawa, M. A topological insulator and helical zero mode in silicene under an inhomogeneous electric field. *New J. Phys.* **2012**, *14*, 033003.

[20] Kane, C.L.; Mele, E.J. Quantum spin Hall effect in graphene. *Phys. Rev. Lett.* **2005**, *95*, 226801.

[21] Min, H.; Hill, J.E.; Sinitsyn, N.A.; Sahu, B.R., Kleinman, L.; MacDonald, A.H. Intrinsic and Rashba spin-orbit interactions in graphene sheets. *Phys. Rev. B* **2006**, *74*, 165310.

[22] Liu, C.C.; Jiang, H.; Yao, Y. Low-energy effective Hamiltonian involving spin-orbit coupling in silicene and two-dimensional germanium and tin. *Phys. Rev. B* **2011**, *84*, 195430.

[23] Barone, V.; Hod, O.; Scuseria, G.E. Electronic structure and stability of semiconducting graphene nanoribbons. *Nano Lett.* **2006**, *6*, 2748-2754.

Figure Captions

Fig. 1. Computed energy band structure of stanene, including spin-orbit coupling effects. The energy gap at the K-point is about 0.1 eV.

Fig. 2. Computed energy band structure of stanene in presence of an out-of-plane electric field E_z of (a) 0.25 V/Å, (b) 0.5 V/Å and (c) 0.75 V/Å.

Fig. 3. Computed energy band gap of stanene as a function of the out-of-plane electric field E_z.

Fig. 4. Atomic structure of a F-passivated Sn armchair nanoribbon (W=6). Blue and orange spheres correspond to Sn and F atoms, respectively.

Fig. 5. Computed energy band gap of Sn nanoribbons as a function of the number of Sn dimer rows along the zig-zag direction. In (a), the calculations do not include SO coupling and are thus indicating the energy gap induced by quantum confinements. In (b), SO coupling is included.

Fig. 6. Energy band structure of F-passivated armchair Sn nanoribbons (including SO coupling), with (a) W=6 and (b) W=8.

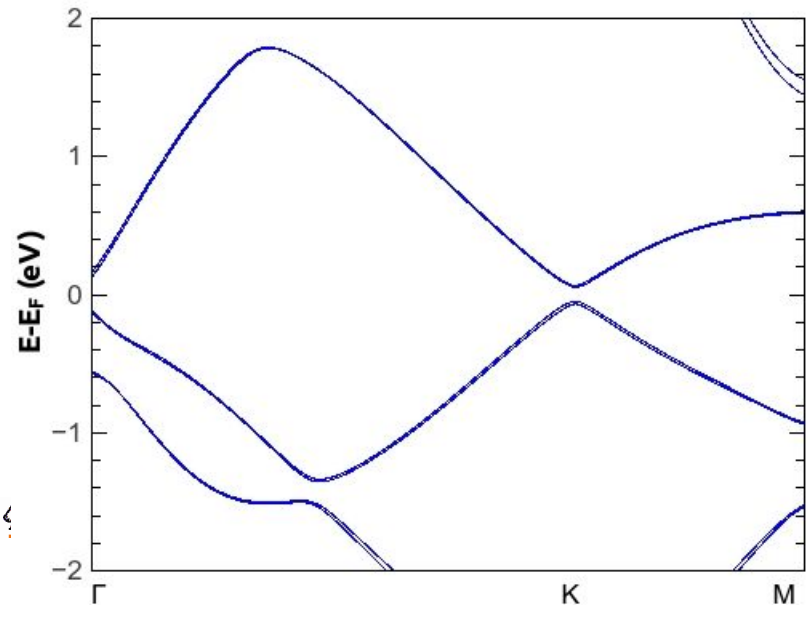

Fig. 1. M. Houssa et al.

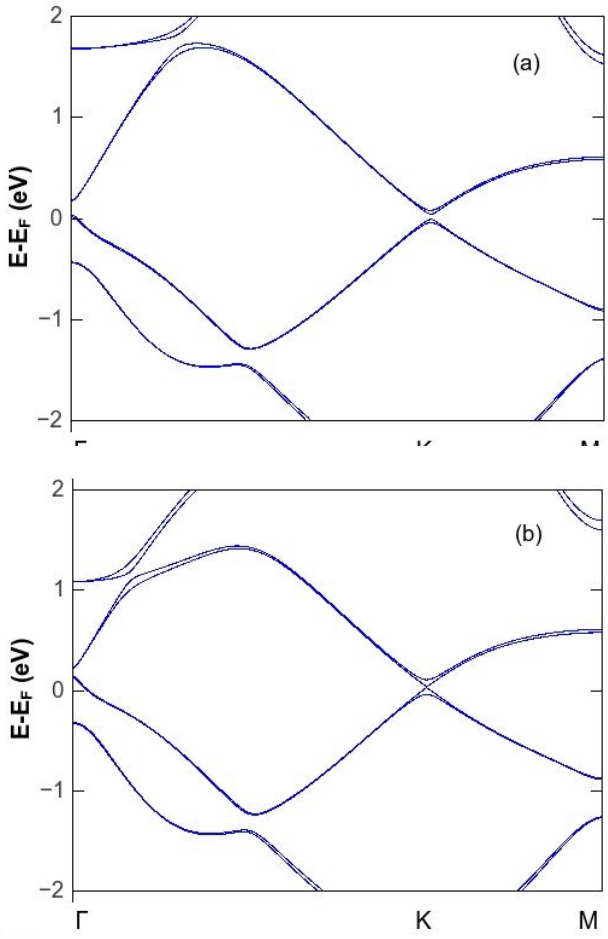

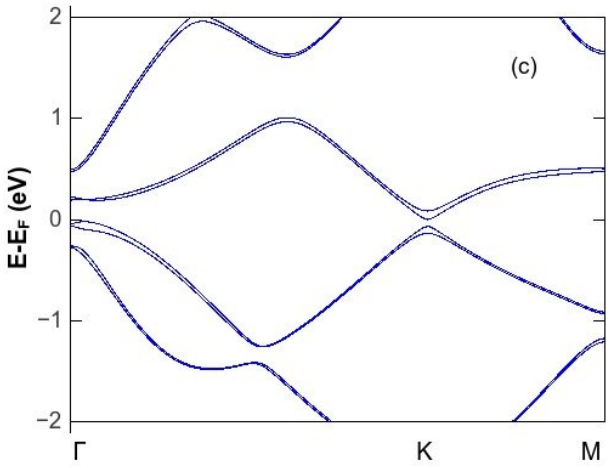

Fig. 2. M. Houssa et al.

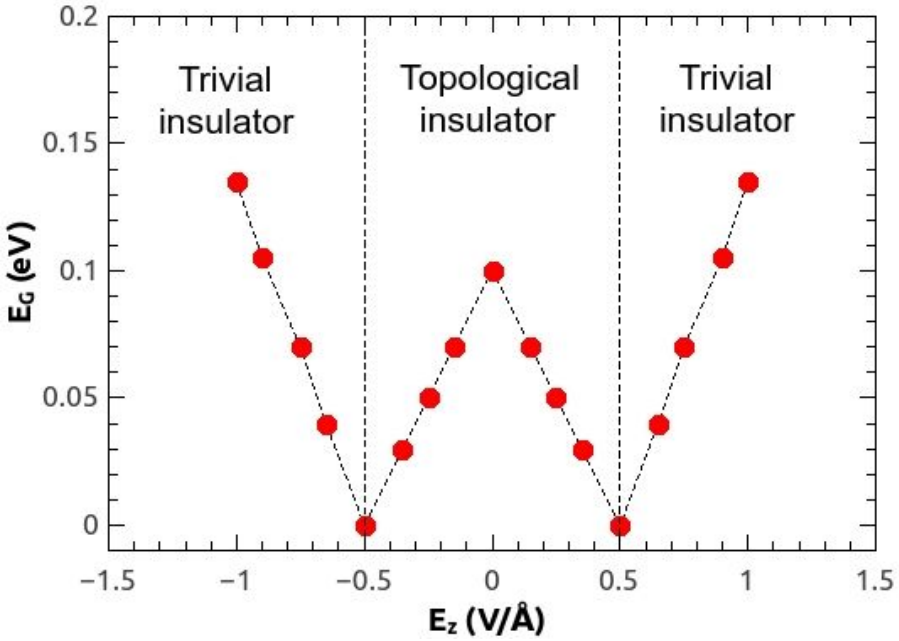

Fig. 3. M. Houssa et al.

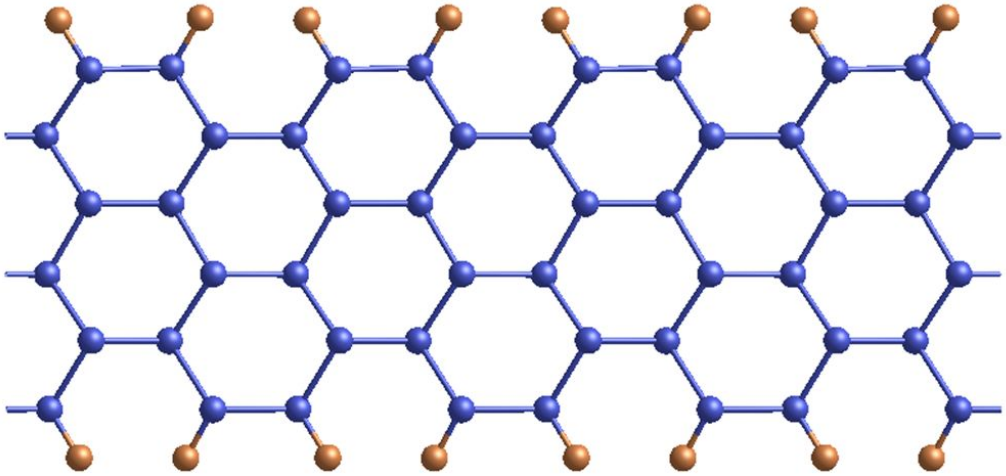

Fig. 4. M. Houssa et al.

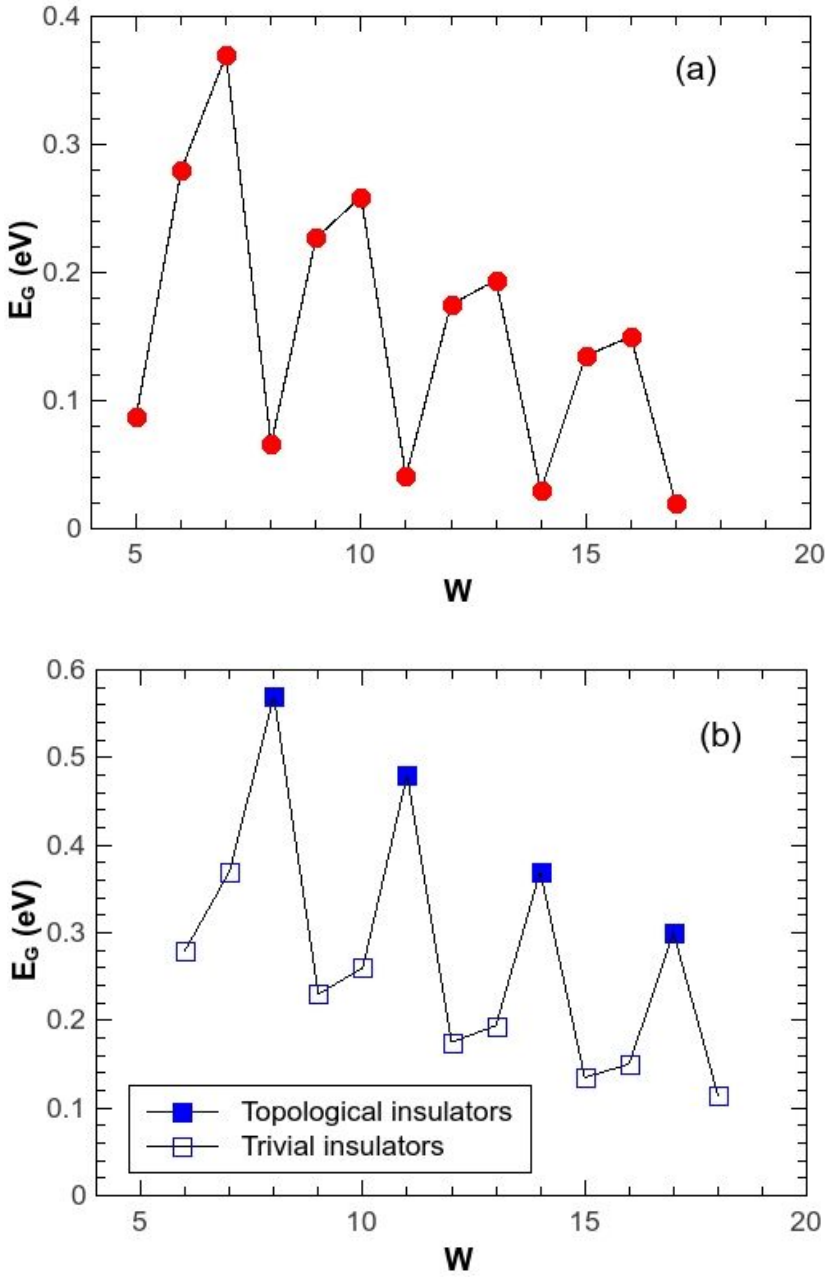

Fig. 5. M. Houssa et al.

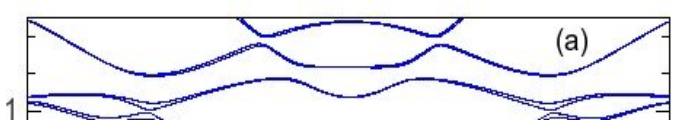

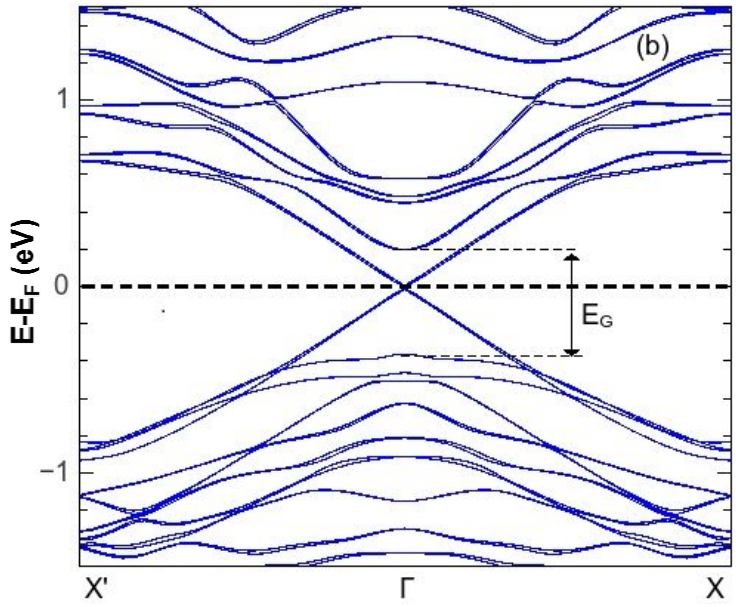

Fig. 6. M. Houssa et al.